

**Distributed self-regulation of living tissue: Beyond the ideal limit**Wassily Lubashevsky,<sup>1,\*</sup> Ihor Lubashevsky,<sup>1,2,†</sup> and Reinhard Mahnke<sup>3,‡</sup><sup>1</sup>*Moscow Technical University of Radioengineering, Electronics, and Automation, Vernadsky 78, 119454 Moscow, Russia*<sup>2</sup>*A.M. Prokhorov General Physics Institute, Russian Academy of Sciences, Vavilov Str. 38, 119991 Moscow, Russia*<sup>3</sup>*Institut für Physik, Universität Rostock, 18051 Rostock, Germany*

(Received 30 November 2008; revised manuscript received 21 January 2010; published 24 February 2010)

The present paper is devoted to mathematical description of the vascular network response to local perturbations in the cellular tissue state, being one of the basic mechanisms controlling the inner environment of human body. Keeping in mind individual organs we propose a model for distributed self-regulation of living tissue, which is regarded as an active hierarchical system without any controlling center. This model is based on the self-processing of information about the cellular tissue state and cooperative interaction of blood vessels governing redistribution of blood flow over the vascular network. The information self-processing is implemented via mass conservation, i.e., conservation of blood flow as well as special biochemical compounds called activators transported by blood. The cooperative interaction of blood vessels stems from the response of individual vessels to activators in blood flowing through them. The general regularities are used to specify the vessel behavior. The arterial and venous beds are considered to be individually of the tree form. The constructed governing equations are analyzed numerically. In particular, first, we show that the blood perfusion rate approximately (in the analyzed case within 10% accuracy) depends only on the local concentration of activators in the cellular tissue. It is due to the hierarchical structure of the vascular network rather than the ideal behavior of individual vessels accepted previously. Second, we demonstrate the distinction between the reaction thresholds of individual vessels and that of the vascular network as a whole. The latter effect is the cause for introducing the notion of activators instead of using such quantities as temperature in describing the living tissue self-regulation.

DOI: [10.1103/PhysRevE.81.021922](https://doi.org/10.1103/PhysRevE.81.021922)

PACS number(s): 87.19.uj, 89.75.Fb, 87.55.dh, 87.19.lr

**I. INTRODUCTION: LIVING TISSUE SELF-REGULATION PROBLEM**

Living multicellular organisms can persist only when their internal temperature, oxygen concentration, glucose level, etc. are in certain tolerance zones, giving rise to a large number of mechanisms controlling these conditions (see, e.g., [1]). When one of such quantities deviates from its normal value and comes close to the boundary of the tolerance zone, the organism has to respond in some way preventing a further variation of this quantity. Biochemical compounds (oxygen, nutrients, etc.) required by cells for their life are transported by blood flow through the vessel system (vascular network). Simultaneously, blood flow withdraws products of their life activity, e.g., carbon dioxide. Let us assume that, for instance, under some circumstances cells in a certain region of a given organ consume an increased amount of oxygen and nutrients. Then, if this region is small enough in comparison with the whole organism blood flow through it just has to grow to maintain the internal environment of the cellular tissue at the appropriate level. This effect will be referred to as the vascular network response to local variations in the state of cellular tissue.

For the further discussion it is necessary to introduce the notion of blood perfusion or, more rigorously, the blood perfusion rate  $\eta(\mathbf{r})$  at a given point  $\mathbf{r}$  in the following way. We

single out all the smallest arteries leading directly to the capillary network, i.e., all the arterioles. Then the tissue space is divided into the collection of disjoint domains (elementary domains)  $\{Q_c\}$  such that these domains together form the tissue space and each of them contains just one arteriole. The given construction enables us to regard an elementary domain  $Q_c$  as the tissue region supplied directly by the corresponding arteriole  $c$  with the required biochemical compounds. We note that the elementary domain introduced in this way has some analogy to the Krogh cylinder used in modeling gas transport in biological organisms (see, e.g., [2]). By definition, the blood perfusion rate  $\eta$  ascribed to a given elementary domain is the amount of blood entering this domain through its arteriole per unit time and divided by its volume. If blood flow is distributed homogeneously on scales of one elementary domain, then we can regard the blood flow rate as a certain continuous field  $\eta(\mathbf{r})$ .

We consider the response of the vascular network to be *perfect* if every cell is supplied with such an amount of oxygen and nutrients that is strictly necessary for its current activity. As a result, if the functioning of a certain tissue region has changed and cells in it need an increased amount of oxygen and nutrients, then the vascular network with perfect behavior is able to deliver the required biochemical compounds to this region in such a manner that blood flow at the other points of cellular tissue not be disturbed at all. However, this requirement is not trivial in the implementation because for blood flow to grow in a certain arteriole it also has to change in larger arteries leading to the given one. In the general case, this blood flow variation in turn induces perturbations of blood flow through the whole vascular network and, as a results, in the other arterioles, neighboring

\*kloom@mail.ru

†ialub@fpl.gpi.ru

‡reinhard.mahnke@uni-rostock.de

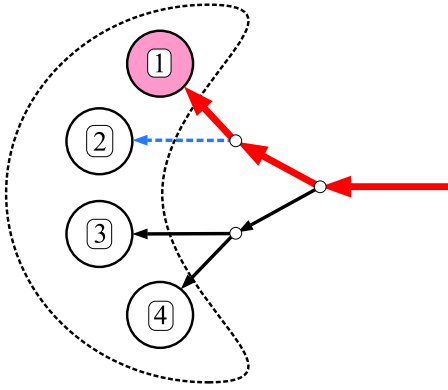


FIG. 1. (Color online) Illustration of interference in the cell functioning caused by the hierarchical structure of the vascular network; intensification of the region 1 activity requiring blood flow to be increased disturbs the blood flow rate in region 2. By thick arrows we note the path on the vascular network with increased blood flow rate, the vessel with the induced decrease in the blood flow rate is marked by dashed arrow, and thin arrows are used to show the vessels with unperturbed blood flow.

and distant ones. Thereby, the vascular network responding to the local need of cells at one point can disturb the functioning of cellular tissue at all its other points, which is illustrated in Fig. 1. This effect, in principle, can give rise to an erratic behavior of the organ as a whole and, thus, should be depressed. Thus, for the vascular network to respond perfectly some mechanism governing the blood flow redistribution over it is necessary.

Since there are no special centers controlling blood flow redistribution on scales of individual organs, their regulation can be implemented only via a cooperative interaction between all its elements. The latter feature allows us to call such regulation processes distributed self-regulation.

Up to now specific mechanisms by which the distributed self-regulation arises are far from being understood well. In order to construct an appropriate model for the distributed self-regulation two aspects must be elucidated. The first one is the self-processing of information because none of the blood vessels possesses the complete information about the state of the corresponding organ. Moreover, each vessel really needs only a piece of information required for its individual functioning. For example, the root artery of a given organ “has nothing to do” with the information about the functioning of a small group of its cells, whereas for an arteriole directly supplying the cells of its elementary domain with nutrients the information about the state of the organ as a whole is redundant. The second aspect concerns the cooperative mechanism governing the blood flow redistribution over the vascular network. None of the vessels control individually blood flow even through itself; responding to the appropriate information it can only dilate or constrict to change its hydrodynamic resistance to blood flow. So the required redistribution of blood flow must be a cumulative effect of their individual actions.

Previously Lubashevsky and Gafiychuk [3–5] proposed a model for the self-regulation of living tissue based on two features. The first one is the hierarchal self-processing of the

information about the system state implemented via conservation of blood flow and the corresponding flow of thermal energy or biochemical compounds caused by the life activity of cells. The second one is the individual response of vessels to the blood temperature or the concentration of these life active products in blood flow going through them. It has been found that there are special conditions under which the living tissue self-regulation is perfect.

Unfortunately, the created model for perfect self-regulation requires an ideal behavior of blood vessels, that is, it holds only within the ideal limit of the vascular network response to local perturbations. In particular, in this limit, the hydrodynamic resistance of vessels to blood flow has to become zero, for example, at some value of the blood temperature. So in reality, it cannot take place, and which properties of this model will hold beyond the scope of the assumption about the ideal vessel behavior has been an open problem. The purpose of the present paper is to develop a model for living tissue self-regulation that does not use this restrictive assumption.

In what follows we will deal mainly with the vascular network response. So to explain the meaning of the further constructions and their relationship with the description of living tissue self-regulation, let us—by way of example—touch on the bioheat transfer problem.

The temperature distribution  $T(\mathbf{r}, t)$  in living tissue heated, for instance, by some external sources is governed by two factors. One of them is the heat diffusion through the cellular tissue. The other can be explained in the following simplified way. Blood in relatively large vessels moves fast enough, so that the heat exchange between it and the cellular tissue is ignorable. Only when blood gets small arterioles and capillaries this heat exchange becomes substantial. As a result, via the arterial bed blood with the body core temperature  $T_a \approx 36.6^\circ\text{C}$  enters the capillary network located in the heated region, where its temperature quickly equilibrates with the temperature  $T$  of the surrounding cellular tissue and, then, it leaves the heated region via the venous bed again without heat interaction with the cellular tissue. This process is effectively described by heat sink with intensity proportional to the blood perfusion rate  $\eta$  [6].

When the tissue temperature comes close to the boundary  $\Delta_T \approx 45^\circ\text{C}$  of the tolerance zone, the blood flow rate  $\eta$  has to grow substantially to prevent further temperature increase, which observed, in particular, for the skin and muscle [7], the ear chamber [8], the prostate [9,10], and the tongue [11]. To take into account this effect in modeling heat transfer in living tissue, it is natural to presume the existence of a certain, may be, functional relationship

$$\eta = \eta\{T\} \quad (1)$$

between the blood perfusion rate and the temperature field  $T(\mathbf{r}, t)$ . The relationship written in the form of local function  $\eta = \eta(T)$  is widely used in modeling hyperthermia treatment (see, e.g., [11–15]). In the frameworks of the ideal vessel behavior [3–5] dependence (1), in fact, takes the form of a local function  $\eta = \eta(T)$  and exhibits strong growth as the tissue temperature comes close to the boundary of the tolerance zone,  $T \rightarrow \Delta_T$ . Namely, for  $T_a < T < \Delta_T$ ,

$$\eta = \eta_0 \frac{\Delta_T - T_a}{\Delta_T - T}, \quad (2)$$

where  $\eta_0$  is the blood perfusion rate under the normal conditions,  $T = T_a$ . Dependence (2) enables us to regard the quantity  $\Delta_T$  as a certain threshold of the living tissue reaction to increase in the tissue temperature, because in its proximity the growth of the blood perfusion rate becomes strongly pronounced. The ideal behavior of individual vessels is discussed in detail in Sec. III; here, we just claim that the quantity  $\Delta_T$  is also the threshold of individual vessel response by the same reasons. However, experiments conducted on thermoregulation in the canine prostate [9,10] demonstrated that the spatial gradient of tissue temperature plays a significant role when the temperature becomes higher than 41 °C. It poses questions as to whether a local dependence  $\eta(T)$  holds for high values of the tissue temperature and what conditions are necessary for this dependence to come into being.

Leaping ahead we note that the living tissue self-regulation has turned out to be approximately perfect due to the hierarchical structure of the vascular network rather than the used assumption about the vessel behavior. So this property practically holds also beyond the ideal limit. Nevertheless when, for example, the tissue temperature comes close to the boundary of tolerance zone, the relationship between the blood perfusion rate and the temperature demonstrates nonlocal effects. In contrast, the reaction thresholds of individual vessels and that of living tissue as a whole become different beyond the scope of the ideal limit. As a result the tissue temperature turns out not to be a proper variable governing explicitly the vessel behavior.

The further structure of the paper is as follows. Section II discusses some facts of human physiology playing the key role in constructing the model. Section III presents in detail the basic features of the distributed self-regulation and explains the difference between the model at hand and the model with the ideal vessel behavior. Section IV just formulates the model under consideration. Section V describes the results obtained by numerical solution of the developed model using the algorithm presented in Appendix B. Finally, Section VI summarizes the key points of the present paper as well as discusses possible generalizations.

## II. PHYSIOLOGICAL BACKGROUND

To justify the key points of the model to be developed let us note the relevant properties of the human physiology referring mainly to textbook [16] with respect to the general features.

### A. Architecture of vessel network

When an organ of human body is active and its tissue needs a greatly increased supply of nutrients, blood flow can locally grow by 20 or 30 times. In contrast, the heart normally cannot increase its cardiac output more than four to seven times greater than when it is at rest. So, dilating or constricting, the blood vessels of each organ have to control *locally* blood flow at the required level.

Figure 2 exhibits the distribution of blood pressure over

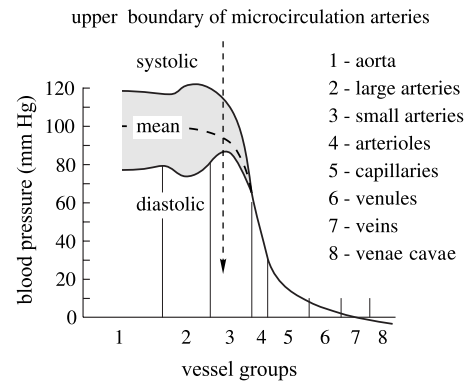


FIG. 2. Schematic illustration of the blood pressure distribution over the vessels of systemic circulation and the roles that various groups of vessels play in blood flow distribution (after [17] with some modification).

the vessels of systemic circulation, which can be classified into “conveying” and “delivering” types [18]. The large vessels, making up the conveying type, maintain a constant value of the mean blood pressure inside the large arteries and damp pressure pulsations via the special mechanism based on the baroreceptors located in the artery walls. As a result, at the entrance to the delivering circulation system of individual organs the blood pressure can be considered as being fixed if the whole organism is not under extreme conditions.

Below the circulation system of an organ comprising small arteries and veins, arterioles and venules together with capillary network will be referred to as a microcirculatory bed. As seen in Fig. 2 the main decrease in the blood pressure falls on the small arteries and arterioles and the blood pressure drop is rather uniformly distributed over many vessels of different lengths. Thereby the net resistance of a microcirculatory bed to blood flow is determined by all its arteries and arterioles rather than vessels of one fixed length.

In general, each artery entering an organ branches six to eight times before the arteries become small enough to be called arterioles, then the arterioles themselves branch two to five times before supplying blood to the capillaries. The arteries and arterioles are highly muscular and their lumen diameters can change many-fold. The branching of these delivering vessels is rather symmetric; the daughter arteries of a mother artery are typically of the same size and form similar angles with the parent vessel.

Microcirculatory beds are typically arranged in a space-filling manner such that the terminal arterioles and venules be distributed in the tissue uniformly. Besides, rather often the layout of their arterial and venous networks is mainly made up of the countercurrent pairs consisting individually of an artery and vein located in space in close proximity to each other. Figure 3 illustrates this countercurrent vessel arrangement. Possible mechanisms of such a pattern formation are discussed, in particular, in [20].

### B. Mechanisms of the tissue self-regulation

To illustrate the state of art we discuss the tissue self-regulation mainly in the brain. In this organ the tissue inner



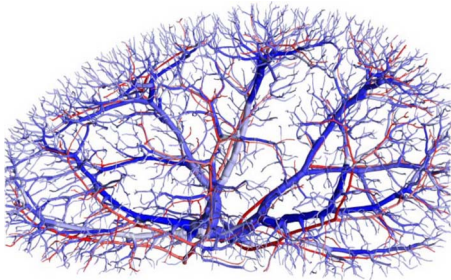


FIG. 3. (Color online) Illustration of the vascular network layout made up of the countercurrent pairs. The figure exhibits the rat renal vasculature reconstructed from computer tomography images (after [19], used with permission).

environment should be controlled by blood flow most effectively and its mechanisms have attracted much attention during the last decade (for a review, see [21–24]).

There is a lot of evidence that the regulation of cerebral circulation is highly localized and cannot be governed *solely* by the products of tissue metabolism (review [25] and references therein). For example, during the local activation of a small region of the brain the corresponding increase in the blood perfusion rate is caused by the dilation of not only small arterioles in it but also relatively large pial arteries that supply directly the activated region with blood [26–28]. On one hand, exactly these arteries offer the greatest resistance to flow and, consequently, are the main site of flow control [29]. On the other hand, the dilated pial arteries lay outside the activated region and, thus, cannot be affected directly by biochemical products of cell activity in it. Thereby, other mechanisms should also contribute to the blood flow regulation. The main hypothesis about these mechanisms noted in many textbooks (e.g., [16]) is based on the release of vasodilator substances such as nitric oxide (NO) by the cells of artery walls. Rapid blood flow through the arteries and arterioles causes shear stress on their cells, inducing the release of NO and finally the vessel dilation. The upstream propagation of this dilation is assumed to be conducted by the cell-to-cell interaction (through homocellular gap junctions with the ions  $\text{Ca}^{2+}$  playing the key role) or just the effect of the successive blood pressure redistribution (e.g., [21]). Yet these models are rather far from being verified well *in vivo* [24], and other mechanisms are under discussion (in particular, [30–34]). Moreover, even the fact of observing *in vivo* upstream coupled waves of  $\text{Ca}^{2+}$  and arteriolar dilation [35] poses a question as to how these waves propagating in both the directions along the arteries pass the points of vessel branching and transfer the information about the cellular tissue states.

The upstream artery dilation can be alternatively caused by artery-vein interaction; for a review, see [36] and, in particular, paper [37] comparing several possible mechanisms with each other as well as work [38] studying this phenomenon in the brain. The main idea is that the downstream transport of biochemical substance with blood flow going through the vein network gives rise to an effective upstream processing of information about the cellular tissue state. The exchange of biochemical compounds between arteries and veins forming countercurrent vessel pairs was assumed to

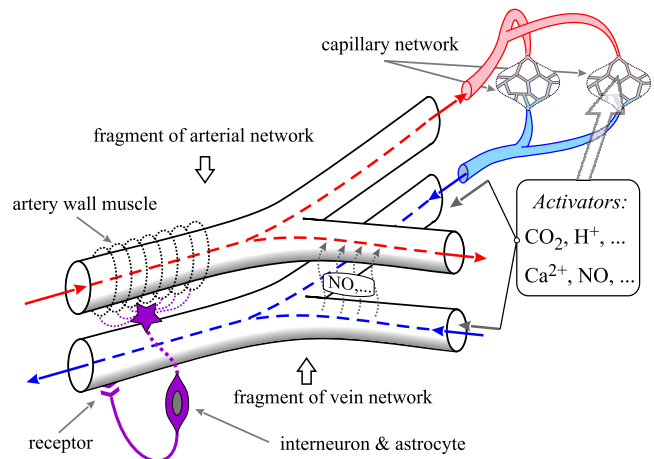


FIG. 4. (Color online) Schematic illustration of physiological processes used in contracting the developed model.

arise via diffusion through the surrounding cellular tissue, being justified theoretically [39,40].

Neural stimuli should also contribute to the *local* regulation of blood flow. In the brain the neural mechanisms of the blood flow regulation are due to the neurovascular units [41–43]. Roughly speaking, the neurovascular unit consists of vessels of microcirculation, interneurons, and astrocytes. Interneurons give rise to short pathways between the tissue cells in the activated region and vessels supplying it with blood. Astrocytes together with interneurons affect the muscles of vessel wall causing dilation or contraction (for details, see [44] and references therein).

The model to be developed actually combines the countercurrent artery-vein interaction and the neural mechanism of local blood flow regulation (Fig. 4). It assumes that the products of cell activity, for example,  $\text{CO}_2$ ,  $\text{H}^+$ , and bioactive substances, including the ions  $\text{Ca}^{2+}$ , NO, etc., are accumulated in the cellular tissue and then with blood enter the vein bed. Below these biochemical substances will be called activators. Receptors embedded into the vein walls detect the concentration  $\Theta$  of the activators in blood flow going through the corresponding veins. Then the “reading” of the receptors are transferred by the neural mechanism to the arteries coupled with these veins, which determines the degree of the artery dilation or contraction. It should be noted that the substance diffusion between the nearest artery and vein can also imitate the action of these receptors.

The next section demonstrates that the proposed mechanism does give rise to the required upstream response of the arteries to the disturbance in the inner tissue environment. Moreover, if this response could be caused by the upstream propagation of some biochemical substance along the arteries that obey conservation at the branching points of the artery tree, then the developed model could also allow for this mechanism after minor modification.

### III. FUNDAMENTALS OF DISTRIBUTED SELF-REGULATION

The two main aspects of distributed self-regulation, i.e., the information self-processing and the vessel response

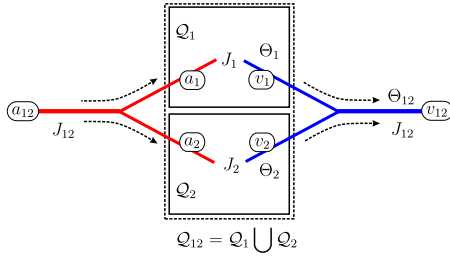


FIG. 5. (Color online) Illustration of the information self-processing caused by mass conservation in the blood flow through the venous bed.

mechanism governing their cooperative interacting in governing blood flow will be discussed individually.

### A. Information self-processing

Figure 5 illustrates the implementation of the self-processing of information about the states of living tissue. Let the activators be uniformly distributed in the domains  $Q_1$  and  $Q_2$  individually with concentrations  $\Theta_1$  and  $\Theta_2$ , respectively. So the values  $\Theta_1$  and  $\Theta_2$  characterize the states of the living tissue in these domains and should determine the response of arteries  $a_1$  and  $a_2$  directly supplying the tissue domains  $Q_1$  and  $Q_2$  with blood transporting oxygen and nutrients. Draining the given domains via the capillary network being in local quasiequilibrium with the surrounding tissue gives rise to the same values of the activator concentrations in veins  $v_1$  and  $v_2$  forming the countercurrent pairs with the arteries  $a_1$  and  $a_2$ . The mass conservation at the shown branching points reads

$$J_{12} = J_1 + J_2, \quad (3)$$

$$J_{12}\Theta_{12} = J_1\Theta_1 + J_2\Theta_2, \quad (4)$$

where  $J_1$ ,  $J_2$ , and  $J_{12}$  are the blood flow rates in these vessels. Whence, it follows that the concentration of activators in the parent vein  $v_{12}$  being equal to

$$\Theta_{12} = \frac{J_1\Theta_1 + J_2\Theta_2}{J_1 + J_2} \quad (5)$$

is the mean values of the activator concentration in the joint domain  $Q_{12} = Q_1 \cup Q_2$  supplied with blood directly by the pair of the artery  $a_{12}$  and the vein  $v_{12}$ . In this averaging the individual blood flow rates  $J_1, J_2$  play role of the weight coefficients. Thereby, the activator concentration  $\Theta_{12}$  is exactly the quantity characterizing the state of the living tissue domain  $Q_{12}$  as a whole and required for the parent artery  $a_{12}$  to respond properly to variations in the state of living tissue in  $Q_{12}$ .

Generalizing this analysis and assuming the mass conservation to hold at all the branching points of the vein bed, we can write

$$\Theta_v = \frac{1}{J_v} \sum_{c \in v} \Theta_c J_c, \quad J_v = \sum_{c \in v} J_c, \quad (6)$$

where  $\Theta_v$  and  $J_v$  are the concentration of activators and the blood flow rate at a given vein  $v$  and the sum runs over all

the venules  $\{c \in v\}$  connected directly with the capillary network and originating from the vein  $v$ . For the sake of simplicity, the terms ‘‘arteriole’’ and ‘‘venule’’ will be used to refer to such smallest arteries and veins connected directly with the capillary network, whereas the terms ‘‘artery’’ and ‘‘vein’’ will be corresponded to the other vessels of arterial and venous beds. Expression (6) gives us the mean value of the activator concentration in the domain  $Q_v = \sum_{c \in v} Q_c$  composed of all the elementary domains (introduced in the Introduction) whose venules originate from the vein  $v$ . It should be noted that the given aspect of the model at hand actually replicates one to one the previous constructions [4] just replacing the blood temperature with the activator concentration.

### B. Description of individual vessel response

The mathematical model of the vessel response assumes the receptors located in the vein walls to detect the presence of activators in the blood going through the corresponding veins by measuring their concentration  $\Theta_v$ . Via the communication between the artery and vein of one countercurrent pair the receptor signal is transmitted to the artery, causing its dilation or contraction to the degree determined by the value  $\Theta_v$ . The higher the concentration, the stronger the artery dilation should be. The effect of artery reaction will be measured in the dependence of its hydrodynamic resistance  $R$  on the activator concentration  $\Theta$  in the coupled vein.

When one of the tissue parameters characterizing its inner environment comes close to the boundary of the tolerance zone, the tissue cells should generate activators to signalize the system about the critical state, causing the blood flow rate to grow. For example, when the tissue temperature  $T$  deviates from the normal value  $T_a = 36.6^\circ\text{C}$  and gets the boundary  $\Delta_T \approx 45^\circ\text{C}$ , the blood flow rate has to increase essentially to prevent the further temperature growth. Let us use the symbol  $\Delta$  to denote the concentration of activators matching such critical situations. In other words,  $\Delta$  specifies the threshold in the individual artery response; when the activator concentration in the coupled vein attains the value  $\Delta$ , the artery has to dilate maximally. The general form of the adopted dependence of the artery resistance  $R$  to blood flow through it on the activator concentration  $\Theta$  in the coupled vein is depicted in Fig. 6 by solid line; the ideal dependence is shown by dotted line. Below as well as in Fig. 6 the activator concentration is measured in the dimensionless units,  $\theta = \Theta/\Delta$ . Figure 6 also justifies the equality of the reaction thresholds of individual vessels and the vascular network as a whole in the approximation of ideal vessel behavior; it was just declared in the Introduction. This figure in its inset depicts the corresponding dependence of the blood perfusion rate on the activator concentration following from expression (2) within the replacement

$$\frac{\Theta}{\Delta} = \frac{T - T_a}{\Delta_T - T_a}. \quad (7)$$

So, in fact, within this approximation the vessel resistance and the blood perfusion rate exhibit strong variations when the value  $\theta$  comes close to the same threshold  $\theta_\Delta = 1$ .

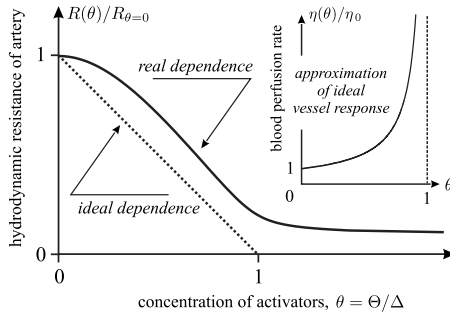


FIG. 6. The resistance of an artery to blood flow through it vs the concentration of activators in the coupled vein. The approximation of the ideal vessel response assumes this dependence to be of the shown linear form and the resulting dependence of the blood perfusion rate on the local value of activator concentration in the cellular tissue is shown in the inset.

In contrast to the mechanism of information self-processing, it only seems that the proposed models for the individual vessel response and the previous one are equivalent within replacement (7). According to the results to be obtained for vessels with nonideal behavior even if their individual resistance can drop by ten times the resulting increase in the blood perfusion rate is not sufficient to affect substantially heat transfer in living tissue when the tissue temperature  $T$  gets its tolerance boundary,  $T = \Delta_T$ . To intensify blood perfusion essentially the tissue temperature  $T$  should exceed the tolerance boundary remarkably, if the vessel behavior were described by the given model within replacement (7). Namely, in this case the estimate  $(T - T_a)/(\Delta_T - T_a) \sim 2$  should hold, giving us the value  $T = 53^\circ\text{C}$ , which cannot take place in the reality. Therefore, coming close to the tolerance boundary  $\Delta_T$ , the tissue temperature is able only to intensify the generation of activators which being accumulated in the cellular tissue cause the vascular network to respond.

#### IV. MODEL OF LIVING TISSUE

The model for the living tissue response to local perturbations consists of three units for the vascular network architecture, the regularities governing blood flow redistribution, and the description of individual vessel behavior.

##### A. Vascular network architecture

The model for the vascular network architecture assumes the following. First, the arterial and venous beds are individually of the tree form [45]. Second, the branching of vessels is symmetrical, i.e., at the branching points of the arterial bed the radii and lengths of daughter arteries are the same as well as are the angles formed by the daughter arteries with their mother artery. A similar statement holds also for the points of the vein merging. Third, the vessels of each level are distributed uniformly in the living tissue domain. This domain is considered to be a square or cube [46].

The first and second assumptions enable us to introduce the vessel hierarchy and to order all the arteries and veins

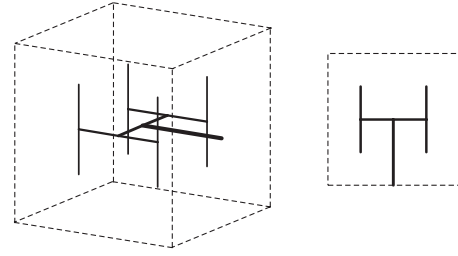


FIG. 7. Dichotomic model of the vessel tree and its characteristic fragments of the embedding into 2D and 3D domains.

according to their position in the hierarchical structure. The arteries and veins reachable from the root artery or vein by passing the same number of the branching points (without return) belong to one level of the hierarchy. All the arteries or veins of one level are identical in properties. In what follows the root vessel will be labeled with index  $n=0$ , the vessels of the next level are labeled with index  $n=1$ , and so on. The third assumption allows us to specify the vessel arrangement in the living tissue domain using a self-similar embedding of the vessels. For example, the length of daughter arteries  $l_{n+1}$  is related to the length  $l_n$  of the mother artery by the ratio  $l_n/l_{n+1} = f$  taking the same value  $f$  for all the levels. Rigorously speaking, this relationship holds only for the transitions between two or three successive levels for two-dimensional (2D) and three-dimensional (3D) models. However, in order to not overload description we will use this statement where it does not lead to misunderstanding. In particular, for the 2D and 3D cases we set  $f_{2D} = \sqrt{2}$  and  $f_{3D} = \sqrt[3]{2}$ , respectively. Figure 7 depicts the characteristic fragment of the vascular network that illustrates the embedding of vessels into the living tissue domain adopted in the present model. The total number of the hierarchy levels (not counting the root vessels) is divisible by 2 or 3 in 2D or 3D cases.

Besides, for the sake of simplicity, the arterial and venous beds are assumed to be the mirror images of each other with respect to all the properties, including the vessel response. This artificial assumption just simplifies the description of the vascular network response to perturbations in the tissue homeostasis. Indeed, the vascular resistance of the real venous beds is small in comparison with that of the arterial beds. Therefore, for a vascular network made up of the counter-current artery-vein pairs the blood flow patterns of the arterial and venous beds should be the mirror images of each other at least approximately. So the latter assumption simply mimics this situation and enables us to speak only about veins and their dilation or contraction in the response to variations in the activator concentration in blood flow through a given vein. Naturally, in order to get the right values of the blood flow rates in this model we have to increase the blood pressure drop across the vascular network twice or, what is the same, to fix formally the pressure inside the cellular tissue equal to the initial pressure at the entrance to the root artery. Figure 8 illustrates the adopted model for the venous bed as well as the mechanism of its response to the variations in the activator concentration in the cellular tissue.



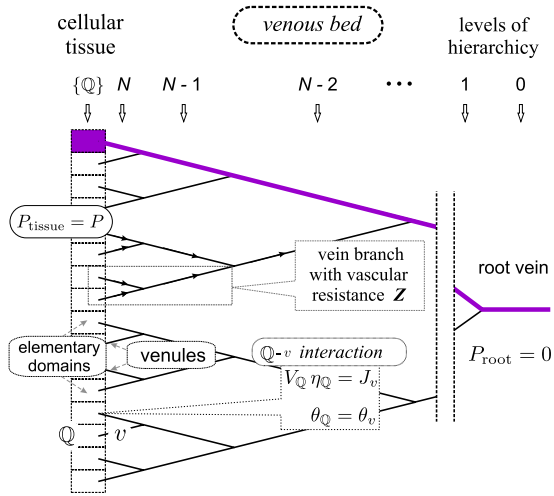


FIG. 8. (Color online) Vascular network model reduced to the venous bed and its reaction to the distribution of activators in the cellular tissue. Here, in particular,  $Q = Q_c$  designates the elementary domain related to the venule  $c$ .

### B. Governing equations for blood flow distribution

The blood flow distribution over the vein network  $\{v\}$  (Fig. 8) is described as follows. First, to every vein  $v$  we ascribe the blood flow rate  $J_v$  and the activator concentration  $\theta_v$  characterizing flow of blood with activators going through it. The state of this vein is quantified in terms of the vessel resistance  $R_n(\theta_v)$  depending on the activator concentration  $\theta_v$  in it, which reflects the vessel response. Here, the function  $R_n(\theta)$  is assumed to be identical for all the vein of one level  $n$ . Second, to every branching point  $k$  we ascribe a certain blood pressure  $P$ . Then the blood flow distribution is governed by the system of equations including Poiseuille's law written for every vein  $v$  (Fig. 9),

$$P_{\text{in}} - P_{\text{out}} = J_v R_n(\theta_v), \quad (8)$$

and conservation of blood and activator substance at every branching point  $k$ ,

$$J_{\text{in},1} + J_{\text{in},2} = J_{\text{out}}, \quad (9)$$

$$J_{\text{in},1} \theta_{\text{in},1} + J_{\text{in},2} \theta_{\text{in},2} = J_{\text{out}} \theta_{\text{out}}. \quad (10)$$

This system of equations should be completed by the “boundary” conditions specifying the blood pressure at the

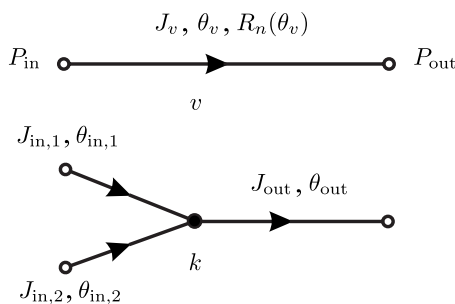


FIG. 9. The main units of the mathematical description of blood flow distribution over the vein bed.

entrance to the venules  $\{c\}$  and the exit from the root vein

$$P_{\text{in}|c} = P, \quad P_{\text{out}|n=0} = 0, \quad (11)$$

and the equality of the activator concentration in every venule  $c$  to the concentration of activators in the corresponding elementary domain  $Q_c$ ,

$$\theta_c = \theta(\mathbf{r}_c), \quad (12)$$

where, for example,  $\mathbf{r}_c$  is the center point of the domain  $Q_c$ . The latter equality assumes the activator distribution in the cellular tissue to be homogeneous on scales of one elementary domain and takes into account that blood flow through capillaries is rather slow and the capillary walls have numerous minute capillary pores permeable to water and other small molecular substances. This gives rise to local equilibrium between blood and the surrounding cellular tissue with respect to the redistribution of biochemical compounds and makes the activator concentration a practically uniform field on scales about the size of elementary domain. In the analysis of the vascular network response the distribution of activators in the cellular tissue is treated as a given beforehand field  $\theta(\mathbf{r})$ .

The desired blood perfusion rate  $\eta(\mathbf{r})$  is calculated actually according to its definition

$$\eta(\mathbf{r}_c) = \frac{J_c}{V_c}, \quad (13)$$

where  $J_c$  is the blood perfusion rate in the venule  $c$  and  $V_c$  is the volume of the elementary domain  $Q_c$ .

Solving the system of equations (8)–(10) subject to conditions (11) and (12) we can find the blood flow rate in the venules  $\{c\}$ . The latter together with expression (13) gives us the desired dependence of the blood perfusion rate  $\eta\{\theta\}$  on the field  $\theta(\mathbf{r})$ .

### C. Regularities of the vessel response

To complete the developed model we should specify the dependence of the hydrodynamic resistance  $R_n(\theta_v)$  of every vein  $v$  on the activator concentration  $\theta_v$  in it. According to the adopted assumptions the value  $\theta_\Delta = 1$  ( $\Delta$  in dimensional units) characterizes the critical conditions when one of the basic tissue parameters comes close to the boundary of tolerance zone. To survive the living tissue has to increase essentially the blood perfusion rate, which is implemented via vessel dilation. Since all the arteries of a microcirculatory bed contribute equally to its vascular resistance each artery should exhaust its ability to widen when the activator concentration exceeds the threshold  $\theta_\Delta = 1$ . This allows us to adopt the following ansatz:

$$R_n(\theta_v) = \rho_n \phi(\theta_v), \quad (14)$$

where  $\rho_n$  is the vessel resistance at  $\theta_v = 0$ , which depends only the number of the hierarchy level and  $\phi(\theta)$  is a certain function universal for all the vessel. Naturally, by definition, at  $\theta = 0$  the equality  $\phi(0) = 1$  holds and for  $\theta \gg 1$  the inequality  $\phi(\theta) \rightarrow \phi_{\text{lim}} \ll 1$  should be the case.

In fact we can use any particular form of the function  $\phi(\theta)$  that gives us the  $R(\theta)$  dependence shown in Fig. 6. This

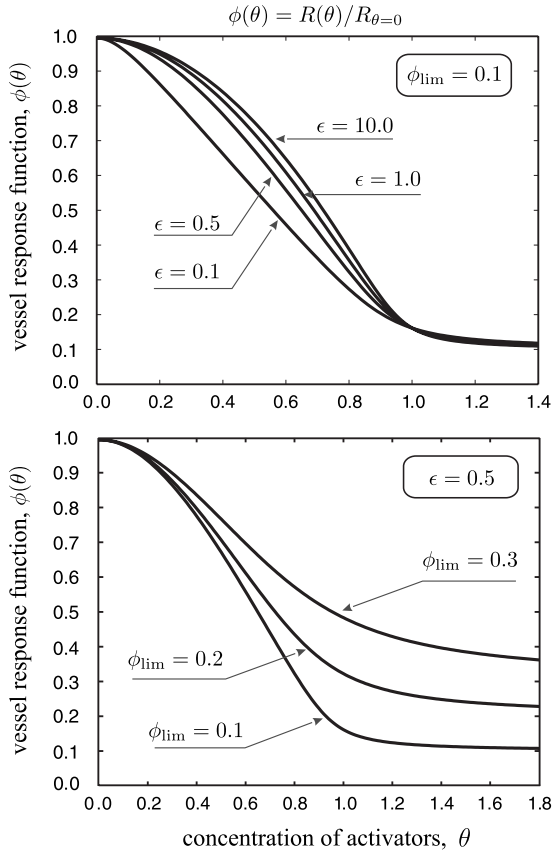


FIG. 10. The vessel response function  $\phi(\theta)$  specified by ansatz (15) for various values of its parameters. The upper fragment exhibits this function for  $\phi_{\text{lim}}=0.1$  and  $\epsilon=0.5, 1.0, 10.0$ . The lower one does it for  $\phi_{\text{lim}}=0.1, 0.2, 0.3$  when the fixed value is  $\epsilon=0.5$ .

function may contain some additional parameters enabling us to analyze, for example, the effect of the maximal vessel dilation on the vascular network response. The following ansatz:

$$\phi(\theta) = \frac{\phi_{\text{lim}} + U(\theta)}{2} + \sqrt{\frac{[\phi_{\text{lim}} - U(\theta)]^2}{4} + 2\phi_{\text{lim}}^2}, \quad (15)$$

where

$$U(\theta) = \frac{1 - \phi_{\text{lim}} - 2\phi_{\text{lim}}^2 \sqrt{\epsilon^2 + 1} - \sqrt{\epsilon^2 + \theta^2}}{1 - \phi_{\text{lim}} \sqrt{\epsilon^2 + 1} - \epsilon}, \quad (16)$$

will be used to be specific. Here, the additional numeric parameter  $\epsilon$  characterizes the linearity of the function  $\phi(\theta)$  in the region  $\theta \lesssim 1$ . Our motivations in constructing expression (15) are presented in Appendix A. Figure 10 visualizes the given function  $\phi(\theta)$  for various values of its parameters. The values  $\epsilon=0$  and  $\phi_{\text{lim}}=0$  match the ideal vessel response. In some sense, ansatz (15) can be justified applying directly to Fig. 10.

The dependence of the vessel resistance on the hierarchy level, i.e., the value of  $\rho_n$  vs the level number  $n$  is constructed using the statement about the equality of contributions to the vascular resistance of arterial beds (Sec. II) from all the hierarchy levels. In other words, when the activator

concentration is the same at all the points of the cellular tissue, in particular,  $\theta(\mathbf{r})=0$ , and thus all the vessels of one level have the same hydrodynamic resistance, the blood pressure drop should be uniformly distributed over the vascular network. This enables us to write the  $\rho_n$  dependence in the form

$$\rho_n = (2\zeta)^n \rho_0, \quad (17)$$

where the value  $\rho_0$  is related with the root vein and the parameter  $\zeta \approx 1$  allows us to consider the cases where various groups of vessels dominate in the blood pressure distribution over the venous bed. In particular, for  $\zeta < 1$  the large veins contribute mainly to the vascular resistance of the vein bed, whereas, in the opposite case,  $\zeta > 1$ , the small veins are dominating.

## V. RESULTS

The blood flow redistribution governed by Eqs. (8)–(10) subject to conditions (11) and (12) was studied numerically using the algorithm described in Appendix B. Variations in the blood flow rate at every vein  $v$  as well as in the blood perfusion rate are analyzed in units of the corresponding quantities,  $I_n$  or  $\eta_0$ , matching the absence of the activators,  $\theta(\mathbf{r})=0$ . These units allow us to reduce the number of the system parameters; only the total number of levels  $N$ , the parameter  $\zeta$  measuring the relative contribution from the large and small vessels to the vascular network resistance, and the parameters  $\epsilon$  and  $\phi_{\text{lim}}$  of the individual vessel response are essential.

The given section presents the results for the 2D system when the activator concentration  $\theta(\mathbf{r})$  differs from zero inside  $m$  first elementary domains located at one of the square corners, namely,

$$\theta(\mathbf{r}) = \begin{cases} \theta, & \mathbf{r} \in Q_\theta := \cup_{1 \leq i \leq m} Q_i \\ 0, & \mathbf{r} \notin Q_\theta. \end{cases} \quad (18)$$

Figure 11 illustrates the analyzed case and shows the introduced ordering of the venules with index  $i$ . The elementary domains are also labeled with the index  $i$  of the corresponding venule.

Figure 12 presents the obtained results. The first column [Figs. 12(a)–12(c)] exhibits the dependence of the blood perfusion rate  $\eta(\theta)$  on the activator concentration  $\theta$  at the same point (through the same elementary domain) of living tissue. In obtaining these results activators were assumed to be located only in the first elementary domain  $Q_1$  [ $m=1$ , except for the case shown in Fig. 12(c)] and the number of the hierarchy levels was set equal to  $N=6$  (but the case shown in the left middle frame). It meets tenfold decrease in the vessels length when passing from the root vessel to the smallest arterioles or venules.

Figure 12(a) depicts three curves corresponding to different values of the parameter  $\zeta$ . When the activator concentration in the domain  $Q_1$  gets the threshold  $\theta_\Delta=1$  of the individual vessel response the venule joined with this domain exhausts its capacity to widen. However, it is not enough for the blood flow rate to grow substantially. Indeed, the contri-



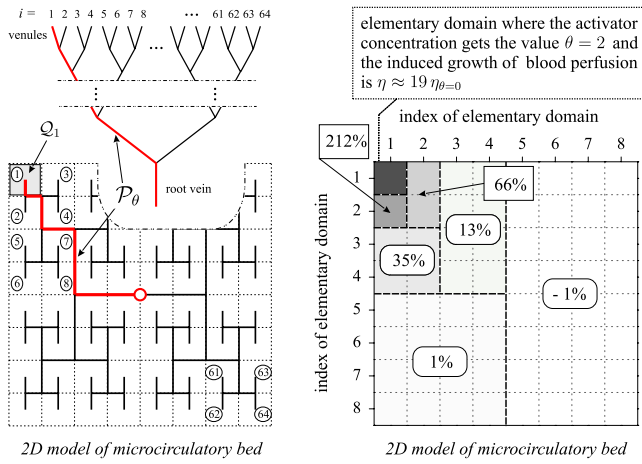


FIG. 11. (Color online) Example of the systems analyzed numerically. The region with a nonzero value of the activator concentration  $\theta$  is shadowed and the ordering of the venules is illustrated for the system with the number of the hierarchy levels equal to  $N = 6$ . The right fragment visualizes the blood flow distribution in the domain of microcirculation bed based on the data obtained numerically and presented in Fig. 12.

bution of this venule to the vascular resistance is small even along the path  $\mathcal{P}_\theta$  leading from the root vessel to the domain  $\mathcal{Q}_1$  on the vein tree (Fig. 11). So many veins along this path have to dilate in order for the blood perfusion rate to grow essentially in  $\mathcal{Q}_1$ . However, the larger a vein, the larger the tissue region drained through this vein as a whole and its size increases exponentially with the number of branching points separating the venule  $v_1$  and the given vein along  $\mathcal{P}_\theta$ . As a result when the activator concentration in the domain  $\mathcal{Q}_1$  is about  $\theta_\Delta = 1$  the activator concentration in relatively large veins on the path  $\mathcal{P}_\theta$  turns out to be rather small and these vessels cannot widen remarkably. Thereby the blood flow rate cannot also exhibit substantial increase (Fig. 12). As the activator concentration grows further the induced increase in the activator concentration along the path  $\mathcal{P}_\theta$  gets the critical value  $\theta_\Delta = 1$  in larger and larger veins, causing the growth of the blood perfusion rate in the domain  $\mathcal{Q}_1$ . When the main part of the veins belonging to  $\mathcal{P}_\theta$  widen to the maximum the blood perfusion rate comes to the upper limit  $\eta_{\max}$ .

The maximum  $\eta_{\max}$  of the blood perfusion rate depends on the system parameter, in particular, on  $\zeta$ . As it will be demonstrated below practically all the additional amount of blood entering the system due to the vessel dilation is directed to the domain  $\mathcal{Q}_1$ . So the higher the contribution of large veins, the higher the upper limit of the blood perfusion rate. These speculations are justified well in Fig. 12(a). Because of this blood flow focusing along the path  $\mathcal{P}_\theta$  the upper limit  $\eta_{\max}$  of the blood perfusion rate can exceed substantially the value  $1/\phi_{\text{lim}}$ , which would be attained if the total blood pressure drop had fallen just on the last vessel supplying the region  $\mathcal{Q}_1$  with blood.

A similar effect should be expected for the dependence of the blood perfusion rate on the number of hierarchy levels. The higher this number, the larger the upper limit  $\eta_{\max}$  of the blood perfusion rate, which is demonstrated directly in Fig. 12(b). When the region of living tissue where activators are

located becomes larger it effectively renormalizes the size of elementary domains and decreases the number of hierarchy levels. So the value of  $\eta_{\max}$  has to drop with  $m$  increasing. The latter behavior is demonstrated in Fig. 12(c), in particular, the value  $\eta_{\max}$  goes down to  $\phi_{\text{lim}}$  when activators spread over the whole region of the microcirculatory bed.

The obtained results demonstrate us also the fact that when the vessel behavior is not ideal the threshold  $\theta_{\text{th}}$  in the vascular network response as a whole does not coincide with the critical value  $\theta_\Delta = 1$  of the individual vessel reaction and can exceed it remarkably. We have treated the threshold  $\theta_{\text{th}}$  as the value of  $\theta$  at which the blood perfusion rate attains one half of its upper limit. Then this fact is clearly visible in Fig. 12(a) and, for example, the estimate  $\theta_{\text{th}} \approx 2$  holds for the case shown by curve 1. Naturally, the threshold  $\theta_{\text{th}}$  depends also on the parameters of the vascular network but not only on the characteristics of individual vessel behavior.

The shown curves enable us to assume that due to the hierarchical structure of the vascular network there is a certain function  $\eta(\theta|\phi, \epsilon)$  depending only on the parameters of individual vessel behavior, which describes the increase in the blood perfusion rate with the growth of the activator concentration until the latter becomes greater than the threshold  $\theta_{\text{th}}$ . The other characteristics of the vascular network and the distribution of activators over the cellular tissue, roughly speaking, affect only the upper limit  $\eta_{\max}$  of blood perfusion rate.

The right column [Figs. 12(d)–12(f)] depicts the distribution of the blood flow rates over the venules. Comparing the data shown here and that of the left column we can declare that the main increase in the blood perfusion rate is located in the region of living tissue containing activators. Exactly these data enable us to assume that the additional amount of blood flow has to be directed mainly along the path  $\mathcal{P}_\theta$ . However, the question about the interference of blood streams induced by distant regions of living tissue requires an individual investigation. Nevertheless, when the living tissue is excited only in one domain its response can be treated as quasilocal. We have used the term “quasilocal” because this response also depends on the size of the excited domain and contains a certain component describing small variations in the blood perfusion rate at distant points.

As the nonlocal component of the  $\eta\{\theta\}$  functional is concerned, Figs. 12(d)–12(f) demonstrate us that depending on the relation between the activator concentration  $\theta$  in the elementary domain  $\mathcal{Q}_1$  and the vascular network threshold  $\theta_{\text{th}}$  it changes its form. When  $\theta < \theta_{\text{th}}$  the increase in the blood flow rate through  $\mathcal{Q}_1$  is caused by the blood flow decrease through the other elementary domains. In this case the required growth of the blood perfusion rate is due to the redistributed of blood flow over the vascular network without additional amount of blood entering the microcirculatory bed. Since the number of the surrounding domains is rather large the decrease in the blood perfusion rate outside the excited region is not essential. When  $\theta > \theta_{\text{th}}$  the increase in the blood perfusion rate is mainly caused by the additional portion of blood entering the microcirculatory bed. Therefore, the blood perfusion rate is increased in the surrounding domains also.

The resulting distribution of the blood perfusion rate in living tissue is shown in Fig. 11 (right fragment) for the 2D

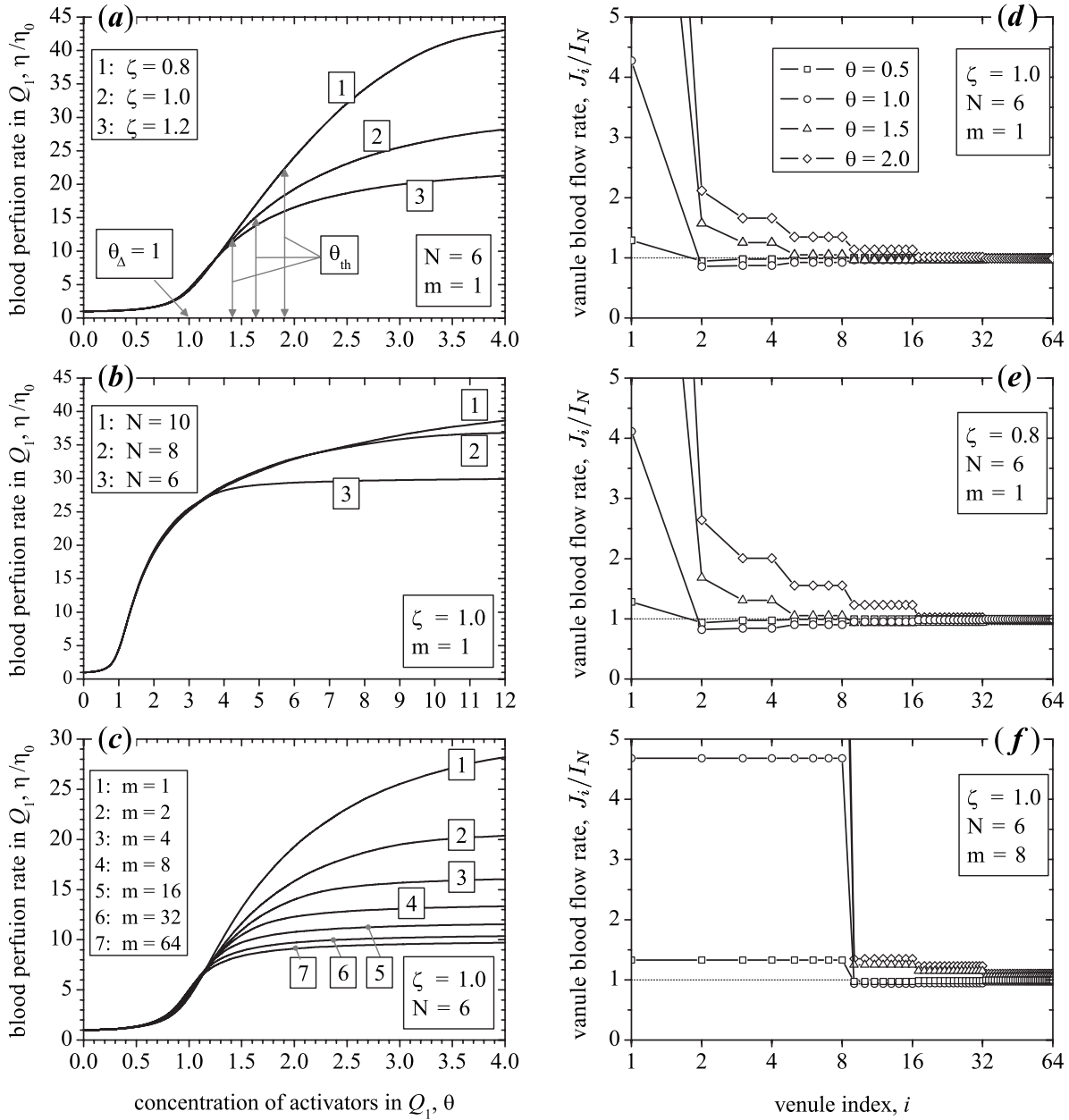


FIG. 12. Results of numerical analysis. Blood perfusion rate  $\eta$  (in units of  $\eta_0$ ) vs the concentration of activators in the same elementary domain  $Q_1$  (left column) and the distribution of the blood flow rates (in units of  $I_N$ ) over the venules, i.e., over the vessels of the last hierarchy level (right column). In obtaining these results the parameters  $\epsilon=1.0$  and  $\phi_{lim}=0.1$  were used; the used values of the other parameters are shown in the figure.

model. As seen the distribution can be rather heterogeneous because the elementary domains neighboring in the physical space can be supplied with blood through the veins (and arterioles) belonging to substantially different branches. If activators are located in another elementary domain the found distribution will also describe this case after a simple reordering of the vessels, whereas in the physical space the blood perfusion pattern can become more heterogeneous than the shown one. The heterogeneity of the blood perfusion rate is caused by the presence of two topologies in the system: one is related to physical space and the other corresponds to the vascular network architecture.

### VI. CONCLUSION AND REMARKS

The paper develops a model for the living tissue as an example of natural complex systems with active behavior. The necessity for such systems to keep their parameters within tolerance zone makes their self-regulation crucial. The absence of local controlling centers in individual organs of the human body poses a question about the mechanism of self-regulation by which the required amount of oxygen and nutrients is delivered to the tissue cell where it is necessary and the equilibrium at the other points is not disturbed.

Keeping in mind the previous papers devoted to this problem [3–5] we have developed a model for a microcirculation

bed (a unit of regional circulation) embedded in 2D and 3D domains of cellular tissue in the self-filling manner. The cells of the tissue continuously require oxygen and various nutrient substances, and the products of their live activity, for example, carbon dioxide, should be withdrawn. When the intensity of cell activity grows the supply of these compounds has to be increased. Exactly this function of the vascular network is under investigation. We have assumed that the necessity for the increased blood supply is signaled by cells via the release of some activators, special biochemical compound.

The artery and vein networks are considered to be of the tree form made up of the artery-vein countercurrent pairs. Activators produced by cellular tissue are withdrawn by blood flow leaving the system via the venous bed. The considered mechanism of living tissue self-regulation is based on two effects. The first one is conservation of blood flow and the amount of activators at the branching points of the vein network. It gives rise to the information self-processing, which is necessary for vessels to respond individually in an adequate way. The hydrodynamic resistance of arteries is determined by the concentration of activators in the blood flow going through the vein forming with a given artery a countercurrent pair. For the sake of simplicity this model is reduced to the description of the venous bed only. The dependence of the vessel resistance on the activator concentration is constructed in a rather general way and deviates substantially from the ideal form analyzed previously [3–5].

The following results have been obtained. First, it is shown that the threshold  $\Theta_{th}$  in the vascular network response to variations in the activator concentration as a whole can differ essentially from the critical value  $\Delta$  of the individual vessel response and is determined not only by the parameters of the vessel behavior but also by the characteristics of the vascular network architecture.

Second, due the hierarchical structure of the vascular network the dependence of the blood perfusion rate on the activator concentration in the cellular tissue is quasilocal. This means that the blood perfusion rate  $\eta(\Theta)$  depends mainly on the activator concentration  $\Theta$  taken at the same point of the living tissue. The prefix “quasi” takes into account that this dependence is affected also by the size of the excited living tissue region. The results of numerical simulation have demonstrated the fact that the  $\eta(\Theta)$  dependence is of a certain universal form determined only by the properties of the individual vessel response for not too high values of the activator concentration,  $\Theta \leq \Delta$ , and only the upper limit  $\eta_{max}$  of the blood perfusion rate is affected by the characteristics of the vascular network architecture and the size of the excited region. It should be reminded that the blood perfusion rate under the normal conditions is treated as a known value. This found quasilocality is explained by the fact that the main part of additional amount of blood going through the system is focused along a path on the vascular network connecting the excited region and the root vessels.

Third, due to the presence of two topologies in living tissue, the point proximity in the physical space and the vessel proximity with respect to their position in the vascular network, the nonlocal component of the functional  $\eta\{\Theta\}$  dependence can be rather heterogeneous in space because

neighboring points of living tissue can be supplied with blood by vessels belonging to vessel branches distant from each other in the vascular network architecture.

### A. Bioheat transfer problem

To demonstrate the relation of the obtained results to the mathematical description of mass and heat propagation in living tissue as an active medium, let us present a model governing the temperature distribution in living tissue heated locally by some external sources  $q_T(\mathbf{r})$ , which allows for the tissue thermoregulation processes.

As noted in Sec. I mass and heat propagation in living tissue is governed by diffusion through the cellular tissue and the blood perfusion playing the role of effective sink with intensity proportional to  $\eta$ . Then using the developed model for the tissue response the governing equations for the temperature distribution can be written as follows:

$$\frac{\partial T}{\partial t} = D_T \nabla^2 T - f_T \eta (T - T_a) + q, \quad (19)$$

$$\frac{\partial \theta}{\partial t} = D_\theta \nabla^2 \theta - f_\theta \eta \theta + g(T). \quad (20)$$

Here,  $D_T$  and  $D_\theta$  are the temperature and activator diffusivities, the coefficients  $0 < f_T, f_\theta < 1$  take into account the heat and mass exchange between arterial and venous blood going through countercurrent artery-vein pairs [47,48] and specified by the vascular network architecture [4], the functional

$$\eta = \eta\{\theta\} \quad (21)$$

describes the living tissue response studied in the present paper, and  $g(T)$  is the dimensionless rate of activator generation. It should be a strongly increasing function as the tissue temperature comes close to the tolerance boundary  $\Delta_T$ .

The system of equations (19) and (20) together with relationship (21) forms a desired model of bioheat transfer in living tissue with thermoregulation. The living tissue response is described by expression (21) within the quasistationary approximation because it is the diffusion through the cellular tissue that limits transient processes in such transport phenomena [4]. The stated model can be also justified appealing to a more detailed description of bioheat transfer problem; see, e.g., reviews [49,50] as well as monograph [4] applying the random walk technique to modeling heat transfer in living tissue where blood flow through vessels forms a fractal network of fast transport paths.

It should be noted that the developed model for the tissue response appeals to the accumulation of the activators in the cellular tissue due to their generation by cells rather than a direct response of blood vessels to the temperature. This can explain the observed delay in the living tissue response to heating [8], which is about ten or more minutes, and grows with the temperature as well as the observed dependence of the tissue response on the temporal gradients of the tissue temperature [9].

### B. Possible generalizations

As possible generalizations of the developed model to systems of other nature concerned, ecological communities and some economical systems should be mentioned. Ecological communities comprising many species continue to exist under environmental perturbations due to complex “predator-prey” relationships maintaining their structure. In particular, in microbial communities predator microorganisms act as regulators to correct microbial imbalances and restore the balanced environment [51]; density-dependent migration sustains the populations of birds, fishes, and insects [52]. Hierarchical organization of ecological communities is based on trophic food pyramids [53] (see also review [54]). Their levels are made up of animals comparable in size and playing much the same role in the prey-predator relationships. The linkages from small organisms generally vary over smaller scales. Larger animals that dominate these smaller organisms do so over larger scales. In such systems variations in species population disturbs locally the prey-predator equilibrium and the induced self-regulation processes should sustain biodiversity [55,56]. Paper [57] proposed a model for an ecological system governed by Lotka-Volterra dynamics, where active individual behavior of the elements at each hierarchical level and self-processing of information enables the system to respond properly to changes in the environment.

In commodity or product markets based on a certain raw material agents of various levels form a trade network and perturbations in the supply-demand equilibrium are damped, in principle, via the reaction of this trade network as a whole. In large companies and distributed technology development the interplay between bottom-up decision making periphery aimed at the overall goals and top-down-driven hierarchical organization can be responsible for self-regulation process (see, e.g., [58,59]). Paper [60] developed a model for self-regulation of a goods market based on a certain raw material. One of its key points is, first, the hierarchical self-processing of the information about the system state that is implemented via conservation of the raw material and money flow at the market network. Second, it is the individual response of firms to disturbance in the local supply-demand equilibrium. In particular, it has been found that there are special conditions under which the self-regulation is perfect.

In both of the two models it was presumed that the ideal behavior of elements is crucial for the self-regulation to be perfect. The results obtained in the present paper enable us pose a general question as to whether the ideal behavior of elements is so necessary for the implementation of perfect self-regulation in active hierarchical systems.

### ACKNOWLEDGMENTS

The authors appreciate the support of DFG Grant No. MA 1508/8-1, RFBR Grants No. 06-01-04005 and No. 09-01-00736, as well as the research support Grant No. R-24-4 from the University of Aizu.

### APPENDIX A: VESSEL RESISTANCE VS ACTIVATOR CONCENTRATION

In order to construct the function  $\phi(\theta)$  let us apply to the following speculations. There should be some threshold  $\epsilon$

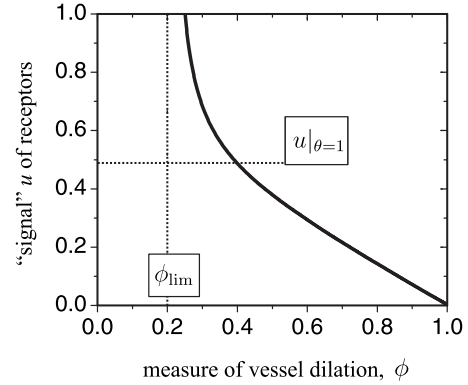


FIG. 13. The expected dependence between the vessel dilation measured in units of  $\phi := R/R_{\theta=0}$  and the receptor signal  $u(\theta)$  caused by activators of concentration  $\theta$ .

$\ll 1$  in the receptor ability to detect activators, meaning that activators cannot be detected if their concentration  $\theta \leq \epsilon$ . So, to be specific, we suppose that the “signal”  $u(\theta)$  generated by the receptors is related to the activator concentration by the ansatz

$$u(\theta) = \sqrt{\theta^2 + \epsilon^2} - \epsilon. \quad (\text{A1})$$

Then the expected relationship between the function  $\phi(\theta)$  quantifying the vessel response and the receptor signal  $u(\theta)$  should be of the form shown in Fig. 13. In particular, as  $u \rightarrow \infty$  the value  $\phi \rightarrow \phi_{\text{lim}}$  and at  $u = u(\theta = 1)$  the vessel dilation should get such a degree that the value  $\phi$  be about its limit; we set  $\phi_{\theta=1} = 2\phi_{\text{lim}}$ . The following ansatz:

$$\frac{1 - \phi_{\text{lim}} - 2\phi_{\text{lim}}^2 u_{\theta=1} - u}{1 - \phi_{\text{lim}} u_{\theta=1}} = \phi - \frac{2\phi_{\text{lim}}^2}{\phi - \phi_{\text{lim}}} \quad (\text{A2})$$

has been chosen to specify this dependence. The combination of expressions (A1) and (A2) yields the final ansatz (15) and (16) for the vessel response function  $\phi(\theta)$ .

### APPENDIX B: NUMERICAL ALGORITHM

The present appendix describes the numerical algorithm used in solving Eqs. (8)–(10). Leaping ahead, we note that the algorithm to be constructed gives us the rigorous solution of these equations, naturally within numerical round-off, by two succeeding iterations: first, from the terminal level  $n = N$  to level  $n = 0$  and, then, in the opposite direction.

In addition to veins we consider the collection of vein branches  $\{B_v\}$ , each of which originates from one of the veins,  $v$ , and contains all its generations (Fig. 14). The hierarchy of branches stems directly from the hierarchy of veins by ordering the branches according to the position of their root vessels in the vein tree. To every branch  $B_v$  we ascribe the resistance to blood flow through it according to the formula

$$Z_v = \frac{P - P_{\text{out}|v}}{J_v}, \quad (\text{B1})$$

just dividing the blood pressure drop across the branch, i.e.,  $P - P_{\text{out}|v}$  (see Fig. 9) by the blood flow rate  $J_v$  at its root vein



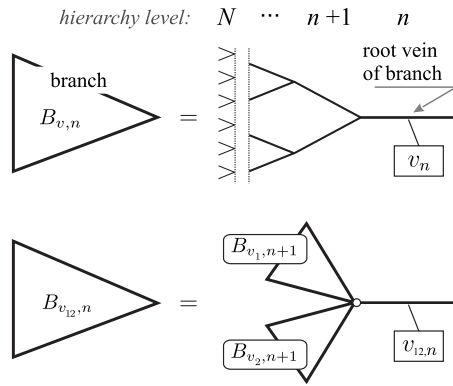


FIG. 14. The structure of a vein branch  $B_{v,n}$  having the vein  $v_n$  as a root vessel (upper line) and the interconnection between the branches of neighboring levels (lower line).

$v_n$ . To every branch  $B_v$  we also ascribe the activator concentration  $\theta_v$  in blood flow going through its root vein  $v$ .

For the venules (veins of the last level) their branches  $\{B_c\}$  consist only of these vessels. So their resistances  $\{Z_c = \rho_N \phi(\theta_c)\}$  can be found directly using condition (12) and expression (14). To pass to the preceding level  $N-1$  we take into account the interconnection between the branches of the neighboring levels shown in Fig. 14. Writing Poiseuille's law for these branches [see expression (B1)] and taking into account mass conservation at the branching point [see expres-

sions (9) and (10)] we, at the first step, can find the activator concentration  $\theta_{12,n}$  in the vein  $v_{12,n}$  from the formula

$$\theta_{12,n} = \left[ \frac{\theta_{1,n+1}}{Z_{1,n+1}} + \frac{\theta_{2,n+1}}{Z_{2,n+1}} \right] \left[ \frac{1}{Z_{1,n+1}} + \frac{1}{Z_{2,n+1}} \right]^{-1}, \quad (\text{B2})$$

if the values  $\{\theta_{n+1}\}$  of activator concentration and the branch resistances  $\{Z_{n+1}\}$  are known at level  $(n+1)$ . Then, at the next step, we calculate the resistance  $Z_{12,n}$  of the branch  $B_{v_{12},n}$  from the equality

$$\frac{1}{Z_{12,n} - R_n(\theta_{12,n})} = \frac{1}{Z_{1,n+1}} + \frac{1}{Z_{2,n+1}}. \quad (\text{B3})$$

In this way all the characteristics of level  $(N-1)$  can be found using these data of level  $N$  and so on up to the root vein of level 0. After reaching the root vein the total blood flow rate  $J_0 = P/Z_0$  is found. Then going in the opposite direction we calculate the blood flow rates  $\{J_1\}$  at level 1 using the equality

$$J_{1(2),n+1} = J_{12,n} \frac{1}{Z_{1(2),n+1}} \left[ \frac{1}{Z_{1,n+1}} + \frac{1}{Z_{2,n+1}} \right]^{-1}, \quad (\text{B4})$$

describing the blood flow split at branching points and so on until getting the venules. At the final step expression (13) gives us the desired dependence of the blood perfusion rate on the distribution of activators in cellular tissue.

- 
- [1] D. D. Chiras, *Human Biology: Health, Homeostasis, and the Environment*, 4th ed. (Jones and Bartlett, Sudbury, Massachusetts, 2002).
- [2] M. H. Friedman, *Principles and Models of Biological Transport*, 2nd ed. (Springer, New York, 2008).
- [3] I. A. Lubashevsky and V. V. Gafiyuchuk, *J. Environ. Syst.* **23**, 281 (1994–1995); *Proc. Russ. Acad. Sci.* **351**, 611 (1996) [in Russian].
- [4] V. V. Gafiyuchuk and I. A. Lubashevsky, *Mathematical Description of Heat Transfer in Living Tissue* (VNTL Publishers, Lviv, 1999).
- [5] I. A. Lubashevsky and V. V. Gafiyuchuk, *SIAM J. Appl. Math.* **60**, 633 (2000).
- [6] H. H. Pennes, *J. Appl. Physiol.* **1**, 93 (1948).
- [7] C. W. Song, A. Lokshina, J. G. Rhee, M. Patten, and S. H. Levitt, *IEEE Trans. Biomed. Eng.* **BME-31**, 9 (1984).
- [8] T. E. Dudar and R. K. Jain, *Cancer Res.* **44**, 605 (1984).
- [9] L. X. Xu, L. Zhu, and K. R. Holmes, *Ann. N.Y. Acad. Sci.* **858**, 21 (1998).
- [10] L. Zhu, L. Pang, and L. X. Xu, *Biomech. Model. Mechanobiol.* **4**, 1 (2005).
- [11] Z. Kai, Z. Yan, C. Ruiqiu, Z. Yufeng, J. Zhihao, Z. Boli, and W. Yi, *Journal of Thermal Biology* **32**, 97 (2007).
- [12] D. T. Tompkins, R. Vanderby, S. A. Klein, W. A. Beckman, R. A. Steeves, D. M. Frey, and B. R. Paliwal, *Int. J. Hyperthermia* **10**, 517 (1994).
- [13] J. Lang, B. Erdmann, and M. Seebass, *IEEE Trans. Biomed. Eng.* **46**, 1129 (1999).
- [14] T. R. Gowrishankar, D. A. Stewart, G. T. Martin, and J. C. Weaver, *Biomed. Eng. Online* **3**, 42 (2004).
- [15] R. S. Cheng, Y. Yuan, Z. Li, P. R. Stauffer, P. Maccarini, W. T. Joines, M. W. Dewhirst, and S. K. Das, *Phys. Med. Biol.* **54**, 1979 (2009).
- [16] A. C. Guyton and J. E. Hall, *Textbook of Medical Physiology*, 11th ed. (Elsevier Inc., Philadelphia, 2006).
- [17] G. I. Kositsky, E. B. Babsky, and A. A. Zubkov, in *Human Physiology*, edited by G. I. Kositsky (Mir Publisher, Moscow, 1990), Vol. 2.
- [18] M. Zamir, *J. Gen. Physiol.* **91**, 725 (1988).
- [19] D. A. Nordsletten, S. Blackett, M. D. Bentley, E. L. Ritman, and N. P. Smith, *Am. J. Physiol. Heart Circ. Physiol.* **291**, H296 (2006).
- [20] A. Al-Kilani, S. Lorthois, T.-H. Nguyen, F. Le Noble, A. Cornelissen, M. Unbekandt, O. Boryskina, L. Leroy, and V. Fleury, *Phys. Rev. E* **77**, 051912 (2008).
- [21] C. Iadecola, *Nat. Rev. Neurosci.* **5**, 347 (2004).
- [22] E. Hamel, *J. Appl. Physiol.* **100**, 1059 (2006).
- [23] J. Lok, P. Gupta, S. Guo, W. J. Kim, M. J. Whalen, K. van Leyen, and E. H. Lo, *Neurochem. Res.* **32**, 2032 (2007).
- [24] C. Iadecola and M. Nedergaard, *Nat. Neurosci.* **10**, 1369 (2007).
- [25] P. Sándor, *Neurochem. Int.* **35**, 237 (1999).
- [26] S. B. Cox, T. A. Woolsey, and C. M. Rovainen, *J. Cereb. Blood Flow Metab.* **13**, 899 (1993).
- [27] J. P. Erinjeri and T. A. Woolsey, *J. Cereb. Blood Flow Metab.* **22**, 353 (2002).

- [28] A. C. Ngai, K. R. Ko, S. Morii, and H. R. Winn, *Am. J. Physiol.* **254**, H133 (1988).
- [29] B. R. Duling, R. D. Hogan, B. L. Langille, P. Lelkes, S. S. Segal, S. F. Vatner, H. Weigelt, and M. A. Young, *Fed. Proc.* **46**, 251 (1987).
- [30] J. L. Jasperse and M. H. Laughlin, *Am. J. Physiol. Heart Circ. Physiol.* **273**, H2423 (1997).
- [31] K. D. Cohen, B. R. Berg, and I. H. Sarelius, *Am. J. Physiol. Heart Circ. Physiol.* **278**, H1916 (2000).
- [32] H. Takano, K. A. Dora, and C. J. Garland, *J. Smooth Muscle Res.* **41**, 303 (2005).
- [33] A. Quan, M. E. Ward, S. Kulandavelu, S. L. Adamson, and B. L. Langille, *J. Vasc. Res.* **43**, 383 (2006).
- [34] K. E. Pyke, J. A. Hartnett, and M. E. Tschakovsky, *J. Appl. Physiol.* **105**, 282 (2008).
- [35] Y. N. Tallini, J. F. Brekke, B. Shui, R. Doran, S. Hwang, J. Nakai, G. Salama, S. S. Segal, and M. I. Kotlikoff, *Circ. Res.* **101**, 1300 (2007).
- [36] R. L. Hester and L. W. Hammer, *Am. J. Physiol. Regulatory Integrative Comp. Physiol.* **282**, R1280 (2002).
- [37] N. R. Harris, G. A. M. First, and R. D. Specian, *Am. J. Physiol. Heart Circ. Physiol.* **276**, H107 (1999).
- [38] K. C. Peebles, A. M. Richards, L. Celi, K. McGrattan, C. J. Murrell, and P. N. Ainslie, *J. Appl. Physiol.* **105**, 1060 (2008).
- [39] M. Kavdia and A. S. Popel, *Am. J. Physiol. Heart Circ. Physiol.* **290**, H716 (2006).
- [40] J. C. Arciero, B. E. Carlson, and T. W. Secomb, *Am. J. Physiol. Heart Circ. Physiol.* **295**, H1562 (2008).
- [41] J. Grotta *et al.*, *Report of the Stroke Progress Review Group* (National Institute of Neurological Disorders and Stroke, Bethesda, Maryland, 2002).
- [42] E. H. Lo, T. Dalkara, and M. A. Moskowitz, *Nat. Rev. Neurosci.* **4**, 399 (2003).
- [43] G. J. del Zoppo and T. Mabuchi, *J. Cereb. Blood Flow Metab.* **23**, 879 (2003).
- [44] C. T. Drake and C. Iadecola, *Brain Lang* **102**, 141 (2007).
- [45] There are special vessels called anastomoses that connect, e.g., arteries belonging to different vessel branches, endowing vascular networks with a more complex topology. Nevertheless, in many organs their relative number is rather low and the presence of anastomoses is of minor importance. The case of high number of anastomoses as it is in the brain requires an individual investigation.
- [46] The chosen shapes of the living tissue domain mimic superficial and volumetric microcirculatory beds having similar dimensions in all the directions. The vascular network of organs with essential asymmetry requires also an individual consideration because it should contain conveying and delivering parts playing different roles in the blood flow redistribution inside the organ.
- [47] S. Weinbaum, L. M. Jiji, and D. E. Lemons, *J. Biomech. Eng.* **106**, 321 (1984).
- [48] L. M. Jiji, S. Weinbaum, and D. E. Lemons, *J. Biomech. Eng.* **106**, 331 (1984).
- [49] M. M. Chen and K. R. Holmes, *Ann. N.Y. Acad. Sci.* **335**, 137 (1980).
- [50] C. K. Charny, in *Advances in Heat Transfer*, edited by Y. I. Cho (Academic, New York, 1992), p. 19.
- [51] R. Mitchell, *Nature (London)* **230**, 257 (1971).
- [52] L. R. Taylor and R. A. Taylor, *Nature (London)* **265**, 415 (1977).
- [53] *A Hierarchical Concept of Ecosystems*, edited by R. V. O'Neill, D. L. de Angelis, J. B. Waide, and T. F. H. Allen (Princeton University Press, Princeton, 1986).
- [54] B. D. Fath and B. C. Patten, *Ecosystems* **2**, 167 (1999).
- [55] B. T. Milne, *Ecosystems* **1**, 449 (1998).
- [56] J. H. Brown, V. K. Gupta, B. L. Li, B. T. Milne, C. Restrepo, and G. B. West, *Philos. Trans. R. Soc. London, Ser. B* **357**, 619 (2002).
- [57] V. V. Gafiychuk, I. A. Lubashevsky, and R. E. Ulanowicz, *Complex Syst.* **11**, 355 (1997).
- [58] S. Valverde and R. V. Solé, *Phys. Rev. E* **76**, 046118 (2007).
- [59] D. Braha and Y. Bar-Yam, *Phys. Rev. E* **69**, 016113 (2004).
- [60] I. A. Lubashevsky, V. V. Gafiychuk, and Yu. L. Klimontovich, *Math. Modell.* **9**, 3 (1997) [in Russian]; *Complex Syst.* **12**, 103 (2000).